

Efficient Implementation of Subcarrier Allocation Schemes in N-Continuous OFDM Transmissions

Enrique M. Lizarraga^{*†}

Victor H. Sauchelli[‡]

Sergio H. Gallina[†]

** Laboratorio de Comunicaciones Digitales - CONICET
emlizarraga@conicet.gov.ar*

*† Universidad Nacional de Catamarca, Argentina
sgallina@tecno.unca.edu.ar*

*‡ Universidad Nacional de Cordoba, Argentina
vsauch@com.uncor.edu*

Abstract— This work presents an efficient implementation of subcarrier allocation schemes in compliance with several orthogonal frequency division multiplexing (OFDM) standards such as LTE. The considered schemes were chosen for OFDM systems owing to its capabilities to overcome certain practical limitations, e.g. improving the required sampling rate or the coding performance. However, they imply an increased computation load based on the large number of subcarriers present in current and future standards. Then it is shown that by means of vector reordering, the fast Fourier transform (FFT) algorithm may be used to avoid the implementation of computationally demanding matrix-vector multiplications derived from the required domain transformation, from frequency to time. The proposed strategy is used in a digital transmitter to obtain a continuous signal, whose first N derivatives are also continuous to reduce the out-of-band power emission. Since a digital signal generation is considered, these results empower hardware reconfigurable applications.

Keywords— N-Continuous, OFDM, LTE, subcarriers, allocation.

1 INTRODUCTION

Orthogonal frequency division multiplexing (OFDM) is an efficient multicarrier modulation which has properties that make it attractive in many high speed communication systems. OFDM is included in many standards such as digital subscriber line (DSL) [1], digital audio broadcasting (DAB) [2], digital video broadcasting (DVB) [3], wireless local area networks (WLAN) [4], and has also been considered for fourth generation (4G) cellular systems such as WiMAX [5] and LTE [6]. OFDM has the attractive ability of compensating the dispersion by means of a simple single-tap equalizer [7] and the use of a cyclic prefix (CP) [8]. Another

important property is the possibility of being implemented by the discrete Fourier transform (DFT) and the efficient algorithms known as fast Fourier transform (FFT) [9].

The OFDM signal is a sequence of OFDM symbols, each one consisting in the modulation of a collection of orthogonal subcarriers. These subcarriers are individually modulated by a conventional complex modulator, e.g. QAM, QPSK. Thus, the phase and amplitude of the subcarriers can be considered to be statistically independent, and also OFDM symbols are statistically independent [8]. In this way the concatenation of OFDM symbols may generate time discontinuities in the signal. In turn, these discontinuities yield high out-of-band energy emission. Current standards use filtering techniques to limit the out-of-band emission despite the fact that this techniques reduce the effectiveness of the CP [10]. In contrast, a novel alternative to reduce out-of-band emissions is proposed in [11], called *N-Continuity*. This technique consists in the use of precoding to force continuity in the signal and its N first derivatives in the limits of every OFDM symbol. One drawback of this alternative is the use of a memory-based precoding since knowledge of two consecutive OFDM symbols is required. Then a complex iterative receiver becomes necessary. Later, this problem was solved in [12], where precoding is turned memoryless by a simple reformulation.

There are two important reasons for selecting a subcarrier allocation scheme with beneficial features. On one hand, to avoid the usage of the central subcarrier allows a sampling rate which is not forced to operate at the symbol rate of the complex modulator of the OFDM system. On the other hand, an allocation scheme with positive and negative frequencies enhances the numerical behavior of the N-continuity algorithm, especially in the case of a large number of subcarriers. Given an appropriate subcarriers allocation scheme, in [12] a theoretical approach to the precoder and the signal obtained is explained. In a previous work we considered a digital signal generator

[13] and showed that the continuity condition can only be correctly represented if oversampling is used in the transmitter.

In this work, we consider the discrete-time signal representation of the continuous-time approach given in [11] and [12]. We develop an algorithm to deal with the desired subcarriers scheme replacing a strong resource-demanding operation by a simpler one, based on the FFT algorithm.

The rest of the paper is organized as follows. In Section 2 a system model and previous works are presented. Section 3 explains the proposed algorithm, and obtained results are shown in Section 4. Finally, conclusions are given in Section 5.

2 SYSTEM MODEL

A conventional continuous-time baseband OFDM signal $s(t)$ is given by

$$s(t) = \sum_i s_i(t - iT), \quad (1)$$

where $s_i(t)$, is the i th OFDM symbol in the i th interval of length T . Every OFDM symbol is obtained as the summation of K orthogonal subcarriers:

$$s_i(t) = \sum_{k=0}^{K-1} d_{i,k} p_k(t) = \mathbf{p}^T(t) \mathbf{d}_i, \quad (2)$$

each one with phase and amplitude determined by the k th complex symbol $d_{i,k}$ obtained from a prior complex modulator. Complex symbols are grouped into the K -element column vector \mathbf{d}_i . The K -element column vector $\mathbf{p}(t)$ contains at each entry the corresponding subcarrier signal $p_k(t)$ given by

$$p_k(t) = e^{j2\pi \frac{k}{T_s} t}; \quad t \in \mathcal{T}. \quad (3)$$

The interval \mathcal{T} is defined by $[-T_g, T_s)$. Cyclic prefix duration is denoted by T_g , and T_s is related to the global symbol rate as K/T_s , consequently $T = T_g + T_s$.

OFDM acceptance was primarily supported by the fact that practical transmitters can obtain the output signal digitally by means of the IDFT instead of deploying K synchronized oscillators. In that case, a sampled version of the output signal without CP can be stated as

$$\mathbf{s}_i = \frac{1}{K} \mathbf{F}^H \mathbf{d}_i, \quad (4)$$

where $\mathbf{F} = \{F_{n,k}\}$ represents the discrete Fourier transform by means of a matrix with elements $F_{n,k} = \exp\left(-\frac{j2\pi kn}{K}\right)$ for $n, k = 0, \dots, K-1$. So, (4) represents the minimum-sampling discrete-time signal for (2), with samples collected in the column vector \mathbf{s}_i .

2.1 N-CONTINUOUS OFDM

As already mentioned in Section 1, one of the most novel approaches to reduce the out-of-band power emission in OFDM systems is N-continuous OFDM

[11]. This technique is supported by a precoder introduced into the conventional OFDM system before the IDFT block of the transmitter. By considering the continuity condition for consecutive OFDM symbols,

$$\left. \frac{d^n}{dt^n} s_i(t) \right|_{t=-T_g} = \left. \frac{d^n}{dt^n} s_i(t) \right|_{t=T_s} \quad (5)$$

is stated for $n = 0, \dots, N$ and for all i . According to [12], a transformation based on an orthogonal projection, and related to the points $t = -T_g$ and $t = T_s$, is possible. Consequently, a $2(N+1) \times K$ constraint matrix

$$\mathbf{B} = \begin{pmatrix} \mathbf{A} \Phi \\ \mathbf{A} \end{pmatrix}, \quad (6)$$

where

$$\mathbf{A} = \begin{pmatrix} 1 & 1 & \dots & 1 \\ k_0 & k_1 & \dots & k_{K-1} \\ \vdots & \vdots & \dots & \vdots \\ k_0^N & k_1^N & \dots & k_{K-1}^N \end{pmatrix}, \quad (7)$$

and $\Phi = \text{diag}(e^{j\phi k_0}, e^{j\phi k_1}, \dots, e^{j\phi k_{K-1}})$ is composed for $\phi = -2\pi \frac{T_g}{T_s}$ and $\{k_0, k_1, \dots, k_{K-1}\} = \{0, 1, \dots, K-1\}$. Finally, an orthogonal projection as defined in [14] is represented by

$$\mathbf{G} = \mathbf{I} - \mathbf{B}^H (\mathbf{B} \mathbf{B}^H)^{-1} \mathbf{B} \quad (8)$$

where \mathbf{I} represents the $K \times K$ identity matrix. Precoded symbols in frequency domain are obtained as

$$\bar{\mathbf{d}}_i = \mathbf{G} \mathbf{d}_i \quad (9)$$

and must be introduced into (2) and (4). For the sake of clarity, we use \mathbf{d}_i instead of $\bar{\mathbf{d}}_i$ in the rest of this work.

3 EFFICIENT IMPLEMENTATION FOR DISCRETE-TIME

Every OFDM symbol is represented in (2) as a summation of continuous-time subcarriers with frequencies corresponding to the set $\mathcal{K} = \{k_0, k_1, \dots, k_{K-1}\}$. As mentioned in Section 1, some constraints in the \mathcal{K} set are introduced in [15]. Then it is defined as

$$\mathcal{K} = \{-K/2, \dots, -1, 1, \dots, K/2\} \quad (10)$$

for $K \in \{300, 600, 900, 1200, 2400\}$.

Although (4) holds for the natural case in the DFT, i.e. $\mathcal{K} = \{0, 1, \dots, K-1\}$, it does not remain valid if (10) is employed. Nevertheless, a matrix-vector multiplication may be used for representing (2) in the discrete-time case. So, it is expressed as

$$\mathbf{s}_i^K = \frac{1}{K+1} \mathbf{Q}^H \mathbf{d}_i^K, \quad (11)$$

where $\mathbf{d}_i^K = (d_{i,0}, \dots, d_{i,K/2-1}, 0, d_{i,K/2}, \dots, d_{i,K-1})^T$, $\mathbf{Q} = \{Q_{n,k}\}$ is a $(K+1) \times (K+1)$ matrix with elements $Q_{n,k} = \exp\left(-\frac{j2\pi \rho_n k}{K+1}\right)$ for $n, k = 0, \dots, K$

and $\boldsymbol{\rho} = \{\rho_n\}$ represents a vector with entries $(-K/2, \dots, -1, 0, 1, \dots, K/2)$.

In order to represent adequately the continuity constraint induced in the precoder, an oversampling factor η is introduced in a previous work of the authors [13]. The oversampled discrete-time signal may be expressed as

$$\mathbf{s}_i^{K\eta} = \frac{1}{K+1} \mathbf{Q}_\eta^H \mathbf{d}_i^K. \quad (12)$$

In this case, $\mathbf{Q}_\eta = \{Q_{\eta n, k}\}$ is a $(K+1) \times (K+1)\eta$ rectangular matrix with elements $Q_{\eta n, k} = \exp\left(-\frac{j2\pi\rho_n k}{K+1}\right)$ for $n = 0, \dots, K$ and $k = 0, \dots, (K+1)\eta - 1$.

Although the previous representation is analytically correct, it is supported by a very high computational load, which may be expressed as $O(K^2\eta)$ in terms of multiplication counts.

Then, we focus on obtaining the discrete-time signal by means of the FFT algorithm. First, a simple transformation is applied on \mathbf{d}_i^K ,

$$\mathbf{u}_i^K = \text{circshift}(\mathbf{d}_i^K, K/2). \quad (13)$$

where $\text{circshift}(\mathbf{a}, b)$ represents a circular up-shifting of b positions applied on the column vector \mathbf{a} . Finally we can state

$$\mathbf{s}_i^K = \text{IFFT}(\mathbf{u}_i^K, K+1), \quad (14)$$

where a b -point inverse fast Fourier transform algorithm applied on the \mathbf{a} vector is represented by $\text{IFFT}(\mathbf{a}, b)$. This representation is numerically equivalent to (11).

Furthermore, the targeted oversampled signal in (12) may be similarly computed as in

$$\mathbf{s}_i^{K\eta} = \eta \text{IFFT}(\mathbf{u}_i^{K\eta}, (K+1)\eta), \quad (15)$$

where $\mathbf{u}_i^{K\eta}$ can be taken as a conventional zero padded version of \mathbf{u}_i^K ,

$$\mathbf{u}_i^{K\eta} = (u_{i,0}^K, \dots, u_{i,K/2}^K, \text{zeros}((K+1)(\eta-1)), u_{i,K/2+1}^K, \dots, u_{i,K}^K), \quad (16)$$

whether $\text{zeros}(a)$ represents an all-zeros column vector with a elements. In this scheme, complexity is derived from the FFT algorithm. If radix-2 is considered, the complexity to compute (15) may be defined by $O\left(\frac{(K+1)\eta}{2} \log_2((K+1)\eta)\right)$. If radix-4 is used, complexity is $O\left(\frac{3}{8}(K+1)\eta \log_2((K+1)\eta)\right)$.

4 RESULTS

4.1 COMPLEXITY COMPARISON

By considering the complexity expressions obtained in the above sections, we analyze some typical settings in standards like IEEE 802.11a/g [4] (64 subcarriers) and IEEE 802.16 [16] (128, 256, 512, 1024, 2048 subcarriers). Digital television systems employ higher subcarrier numbers [3]. Note that the mentioned settings are constrained to be a power of two (or four). However,

N-continuity is focused on LTE, where the specified subcarriers numbers are 300, 600, 900, 1200 and 2400. Since the efficient implementation considered in this work is based on the radix-2 and radix-4 FFT algorithms, an IFFT calculation with additional points is necessary, then K_{min} points are indicated. In this situation, complexity depends on K_{min} , which is defined by the minimum power of two (or four) greater than the specified subcarriers count in the standard.

For a radix-2 implementation of FFT, complexity is drawn in Fig. 1 where oversampling is omitted ($\eta=1$). The complexity obtained with the matrix-vector multiplication discrete-time signal generation is also plotted. For the considered LTE parameters, complexity is indicated by circles in Fig. 1. Note that complexity is

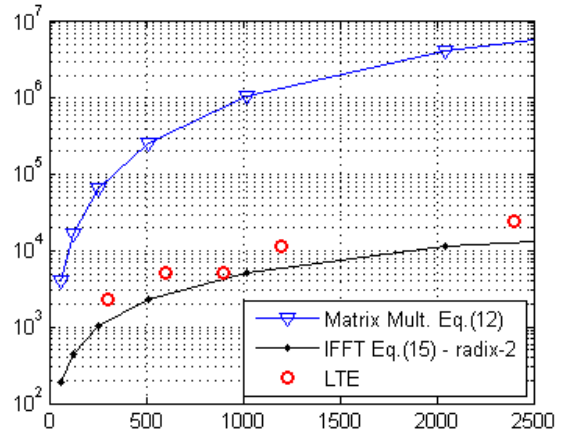


Figure 1: Complexity in logarithmic scale for various values of K , $\eta=1$. Radix-2.

strongly reduced by means of the FFT approach. Even in the case of LTE settings where a calculation with a length greater than the necessary is used, an improvement is still shown. In Fig. 2 we plot the complexity ratio for the LTE configurations, where the measure

$$\frac{\frac{(K+1)\eta}{2} \log_2((K+1)\eta)}{\frac{K_{min}\eta}{2} \log_2(K_{min}\eta)} \quad (17)$$

is taken. Then, complexity ratio is approximately 50%, except for $K=900$, where $K_{min}=1024$ and efficiency is enhanced by the closeness of both values. In turn, Fig. 3 and Fig. 4 represent the obtained behavior with the radix-4 algorithm. In this case, complexity ratio is similarly defined as

$$\frac{\frac{3}{8}(K+1)\eta \log_2((K+1)\eta)}{\frac{3}{8}K_{min}\eta \log_2(K_{min}\eta)}. \quad (18)$$

Based on this, Fig. 4 exhibits a penalty for $K=300$ and $K=1200$. It derives from the big difference between the possible IFFT lengths in the radix-4 alternatives, compared to the required one.

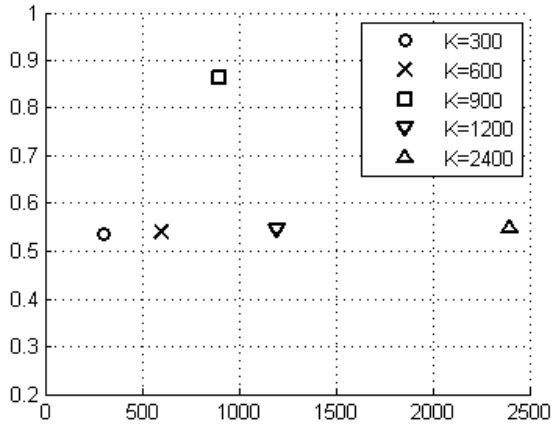


Figure 2: Complexity ratio for various values of K in LTE, $\eta=1$. Radix-2.

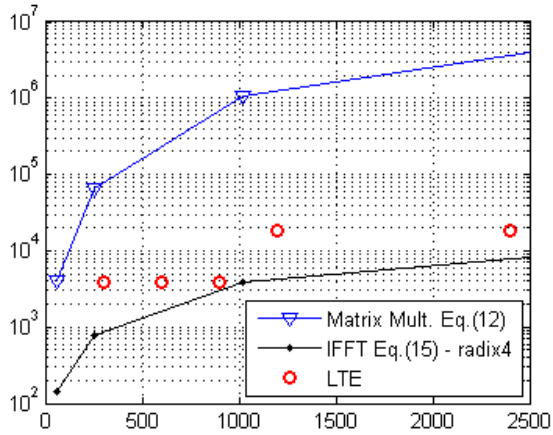


Figure 3: Complexity in logarithmic scale for various values of K, $\eta=1$. Radix-4.

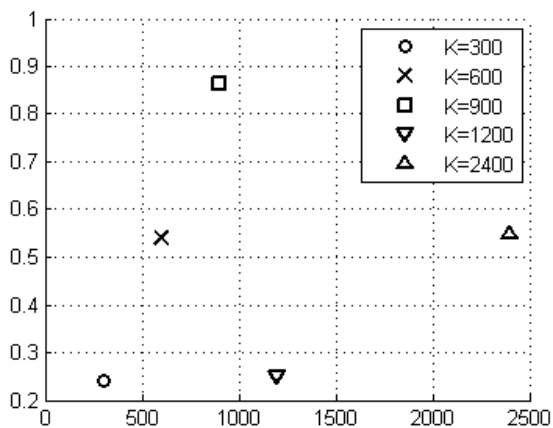


Figure 4: Complexity ratio for various values of K in LTE, $\eta=1$. Radix-4.

When oversampling is considered, a different K_{min} must be found. Based on the requirement of 8192 samples for an OFDM symbol with 600 subcarriers, η is fixed at 14. Complexity is presented in Fig. 5 for radix-2, and its complexity ratio is shown in Fig. 6. By considering radix-4 algorithm, Fig. 7 and Fig. 8 are included. Complexity ratios for both radix-2 and radix-4 present a pattern similar to the achieved with $\eta=1$. Nevertheless, absolute values for the complexity ratios show a diminished performance. In this case the proposed approach is still less complex than the matrix multiplications alternative (see Fig. 5 and Fig. 7).

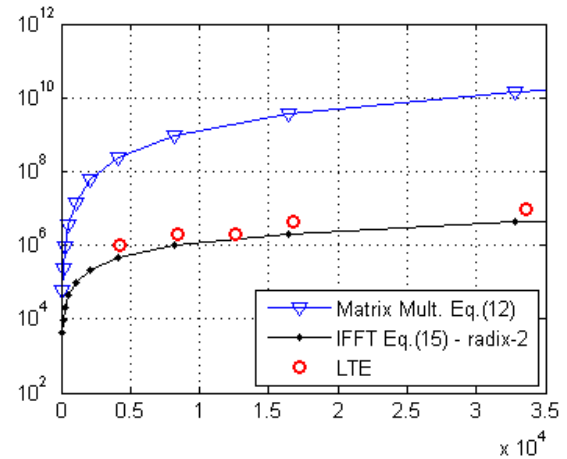


Figure 5: Complexity in logarithmic scale for various values of K, $\eta=14$. Radix-2.

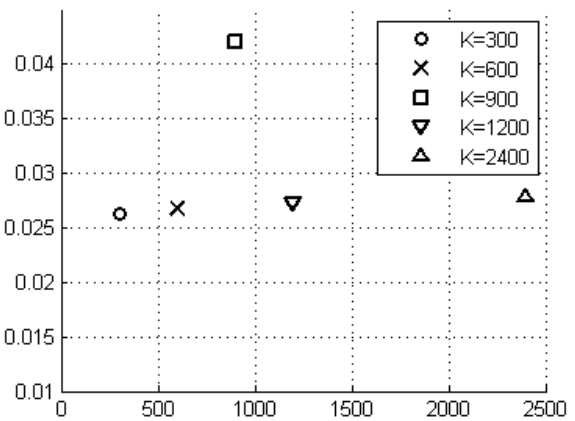


Figure 6: Complexity ratio for various values of K in LTE, $\eta=14$. Radix-2.

4.2 NUMERICAL SIMULATION

The calculation an oversampled discrete-time signal with the subcarriers allocation scheme described before is addressed in this work. The output signal must be compliant with the LTE standard. Also, digital

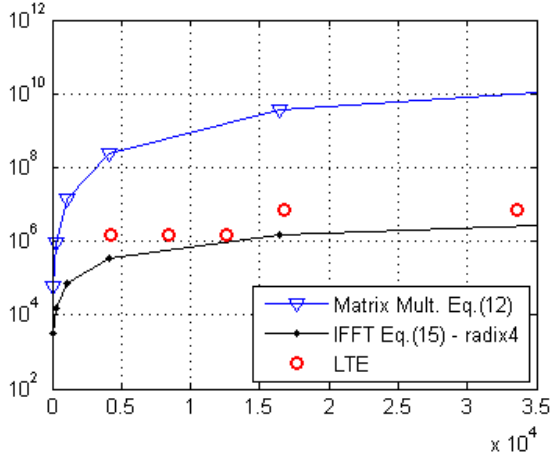


Figure 7: Complexity in logarithmic scale for various values of K , $\eta=14$. Radix-4.

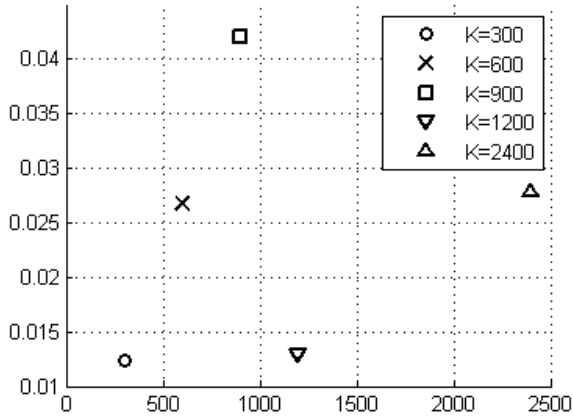


Figure 8: Complexity ratio for various values of K in LTE, $\eta=14$. Radix-4.

signal generation is considered. Then, an additional requirement is achieving a good numerical behavior for the N-Continuity precoding. In this context, spectral performance for the complete system is given in this section.

An OFDM transmission with $K=600$ subcarriers is selected, where $\mathcal{K} = \{-300, \dots, -1, 1, \dots, 300\}$. A 16-QAM complex modulation is employed and an equal portion of 46 dBm total average power is assigned to each subcarrier. Timing is defined by $T_s = \frac{1}{15}$ ms and $T_g = \frac{9}{128} T_s$. A sampling time $T_{sample} = \frac{T_s}{8192}$ is used. Power spectra are estimated by Welch's averaged periodogram method with a 8192-sample Hanning window and a 1024-sample overlap for a 1 sec. observation time. Results are given in Fig. 9, where different curves indicate the performance for continuity orders ranging from 0 to 3, and the conventional case (without N-Continuity). In Fig. 9, continuous lines represent the performance of the proposed algorithm while dashed lines correspond to the ma-

trix multiplication approach. It is showed an identical behavior for both methods, matrix- and FFT-based.

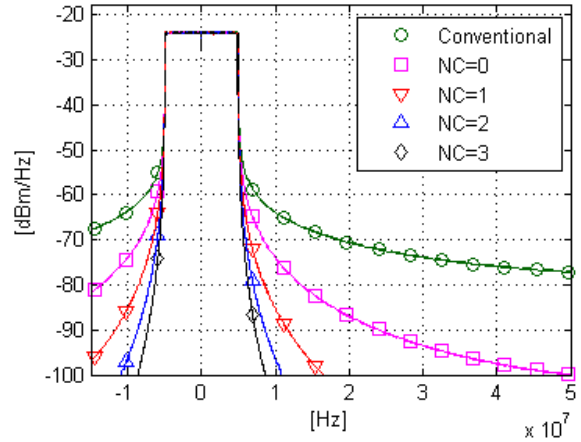


Figure 9: Spectrum for various values of N .

Finally, symbol error rate (SER) performance is presented in Fig. 10 for different signal-to-noise ratios. A conventional Rayleigh channel is considered. A finite impulse response with 42 taps represents the channel. Gaussian noise with zero mean is employed. Settings in this simulation defined 120000 complex symbols. The picture refers to a high distortion case where $N = 3$. According to [15, 12], error-vector magnitude (EVM) is higher in this situation, compared to lower N settings. It is observed that the curve slope is not affected by SNR values less than 35 dB. However, the last point in the curve suggest the presence of an error floor, which is similar to the results in [11]. Nevertheless, a good performance is achieved.

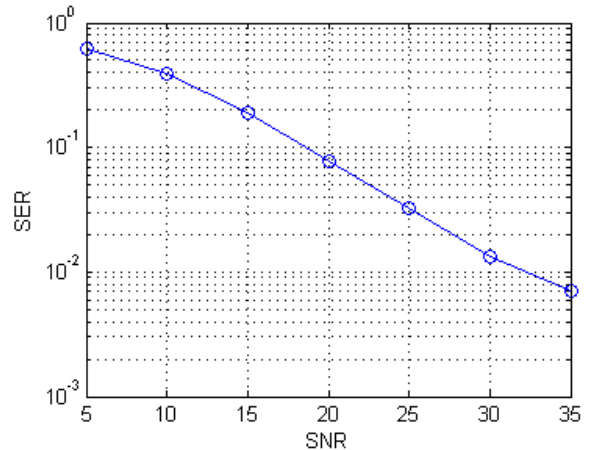


Figure 10: Symbol error rate for a Rayleigh fading channel, $N=3$.

5 CONCLUSIONS

Efficient implementation of subcarriers allocation schemes as defined in LTE is considered. These sub-

carriers mapping strategies allow enhancing the performance of the analog-to-digital converter at the receiver. Also, an improved numerical behavior of the N-Continuity precoder may be achieved. However, if digital signal generation is considered, the matrix-vector multiplication approach to implement the domain transform requires a large computation load. In this context, an FFT-based algorithm is proposed, and its reduced complexity with equivalent performance is shown.

REFERENCES

- [1] *Asymmetric Digital Subscriber Line (ADSL) Metallic Interface*, ANSI Std. ANSI/TIEI/9J-007, 1997.
- [2] *Radio Broadcasting Systems: Digital Audio Broadcasting (DAB) to Mobile, Portable and Fixed Receivers*, ETSI Std. ETS 300 401, 1.3.2 ed., 2000.
- [3] *European Broadcasting Union, Digital Video Broadcasting (DVB); Framing Structure, Channel Coding and Modulation for Digital Terrestrial Television*, ETSI Std. EN 300 744 V1.4.1, 2001.
- [4] *IEEE Part 11: Wireless LAN Medium Access Control (MAC) and Physical Layer (PHY) Specifications: High-Speed Physical Layer in the 5 GHz Band*, IEEE Std. IEEE Std. 802.11a-1999, 1999.
- [5] "Draft Amendment to IEEE Standard for Local and Metropolitan Area Networks Part 16: Air Interface for Fixed and Mobile Broadband Wireless Access Systems: Improved Coexistence Mechanisms for License-Exempt Operation (Amendment to IEEE 802.16-2004)," *IEEE Unapproved Draft Std P802.16h/D6*, May 2008.
- [6] *Evolved Universal Terrestrial Radio Access (E-UTRA); Physical Channels and Modulation (Release 8)*, 3GPP TSG RAN TS 36.211 Std. v8.4.0, Dec. 2008. [Online]. Available: <http://www.3gpp.org/>
- [7] J. Cimini, L., "Analysis and Simulation of a Digital Mobile Channel Using Orthogonal Frequency Division Multiplexing," *IEEE Transactions on Communications*, vol. 33, no. 7, pp. 665 – 675, Jul. 1985.
- [8] R. van Nee and R. Prasad, *OFDM for Wireless Multimedia Communications*. London, UK: Artech House, 2000.
- [9] S. Weinstein and P. Ebert, "Data Transmission by Frequency-Division Multiplexing Using the Discrete Fourier Transform," *IEEE Transactions on Communication Technology*, vol. 19, no. 5, pp. 628 –634, 1971.
- [10] M. Faulkner, "The Effect of Filtering on the Performance of OFDM Systems," *IEEE Transactions on Vehicular Technology*, vol. 49, no. 5, pp. 1877 –1884, Sep. 2000.
- [11] J. van de Beek and F. Berggren, "N-continuous OFDM," *Communications Letters, IEEE*, vol. 13, no. 1, pp. 1 –3, 2009.
- [12] J. van de Beek and F. Berggren, "EVM-constrained OFDM precoding for reduction of out-of-band emission," in *Vehicular Technology Conference Fall (VTC 2009-Fall), 2009 IEEE 70th*, 2009, pp. 1 –5.
- [13] E. M. Lizarraga, V. H. Sauchelli, and G. N. Maggio, "N-continuous OFDM Signal Analysis of FPGA-based Transmissions," in *IEEE Southern Conference on Programmable Logic (SPL) 2011*, Apr. 2011, pp. 13 –18.
- [14] G. Strang, *Linear Algebra and its Applications, 3rd ed.* San Diego, CA: Harcourt Brace Jovanovich Publishers, 1976.
- [15] *Base Station (BS) Radio Transmission and Reception (Release 8)*, 3GPP TSG RAN TS 36.104 Std. v8.4.0, Dec. 2008. [Online]. Available: <http://www.3gpp.org/>
- [16] *IEEE Standard for Local and metropolitan area networks Part 16: Air Interface for Broadband Wireless Access Systems*, IEEE Std. IEEE Std. 802.11a-1999, 2006.